

Defect Perovskites in the $\text{Sr}_{1-x}\text{M}_{1-2x}\text{Nb}_{2x}\text{O}_3$ ($M = \text{Ti}, \text{Zr}$) Family

W.R. Brant and S. Schmid

School of Chemistry, The University of Sydney, NSW, 2006, Australia.

A number of samples have been synthesised in the $\text{Sr}_{1-x}\text{Ti}_{1-2x}\text{Nb}_{2x}\text{O}_3$ system within the composition range $0 < x \leq 0.6$ and investigated using synchrotron X-ray powder diffraction data. The symmetry was found to remain cubic $Pm\bar{3}m$ across the solid solution range $0 \leq x \leq 0.2$ and for temperatures between 90 and 1248 K. Whereas the $\text{Sr}_{1-x}\text{Ti}_{1-2x}\text{Nb}_{2x}\text{O}_3$ system intercalated $\sim 0.075(1)$ mol of lithium chemically the analogous $\text{Sr}_{1-x}\text{Zr}_{1-2x}\text{Nb}_{2x}\text{O}_3$ system was able to intercalate up to 0.5 mol of lithium electrochemically.

1. Introduction

Compounds that can reversibly intercalate lithium have the potential to be used as cathodes in rechargeable lithium ion batteries. Two characteristics of cathode materials, the availability of interstitial or defect sites for the incorporation of lithium and the presence of reducible cations able to accept electrons from an external circuit, are found in some A-site deficient perovskites.

The Sr_xNbO_3 , $0.7 \leq x \leq 1$, solid solution having niobium in both oxidation states +IV and +V whenever $x < 1$, has been reported to adopt the ideal cubic perovskite structure across the whole solid solution field. Despite intensive searching when data were collected on good quality single crystals no additional reflections were detected [1]. This indicates random ordering between strontium and vacancies on the perovskite A sites. Given the vacancies in the structure (particularly at the low strontium end of the solid solution) and the accompanying presence of niobium +V, which can be easily reduced by lithium metal, this solid solution appeared to be an interesting candidate to investigate lithium intercalation properties. As niobium +IV is not stable at high temperatures in air but rather gets oxidised, previous syntheses of the solid solution were conducted in high vacuum. Substitution of all niobium +IV by zirconium +IV or titanium +IV allows syntheses to be carried out in air.

An investigation was undertaken in the $\text{SrO-ZrO}_2\text{-Nb}_2\text{O}_5$ system to see whether an analogous solid solution is indeed formed, what the extent of the solid solution range is and whether this material has the potential to intercalate lithium ions reversibly. The composition range was established as $\text{Sr}_{1-x}\text{Zr}_{1-2x}\text{Nb}_{2x}\text{O}_3$, $0 \leq x \leq 0.28$, and the resulting structures characterised using high resolution neutron powder diffraction data. While structures in this composition range are closely related to the cubic perovskite parent the symmetry for all investigated compositions is lowered to tetragonal or orthorhombic. For $x < 0.15$ the resulting space group is tetragonal $I4/mcm$, for $x > 0.15$ it is orthorhombic $Pnma$ and for $x = 0.15$ two phases co-exist, in space groups $I4/mcm$ and $Imma$ [2].

The aim of this study is to synthesise a number of defect perovskites for the analogous titanium system and investigate their structures using synchrotron X-ray powder diffraction. In addition the chemical and electrochemical lithium intercalation properties of the two systems will be investigated and compared.

2. Experimental Method

Polycrystalline samples of several members of the $\text{Sr}_{1-x}\text{Ti}_{1-2x}\text{Nb}_{2x}\text{O}_3$ ($0 < x \leq 0.6$) series were prepared via conventional solid state reactions. Stoichiometric amounts of the starting materials SrCO_3 , TiO_2 and Nb_2O_5 were finely ground in acetone using a mortar and pestle.

The powder samples were heated at 1100 °C for 15 hours then pressed into pellets and fired at 1300 °C for a further 24 hours, 48 hours and 72 hours with intermittent re-grinding. The reaction progress was monitored using a PANalytical X'Pert PRO MPD X-ray diffractometer set up in Bragg PDS mode, equipped with a PIXcel detector using $\text{Cu}_{K\alpha}$ radiation. Subsequent synchrotron X-ray analysis was carried out on samples in the range $0 < x \leq 0.2$.

High resolution synchrotron X-ray diffraction patterns were collected on the powder diffraction beamline, 10-BM, at the Australian Synchrotron using the MYTHEN microstrip detector [3] and a Si(111) monochromator that accepts the beam directly from a bending magnet source. Using LaB_6 (NIST standard 660a) the wavelength was accurately refined. Samples for collection at room temperature and low temperature were packed into 0.3 mm glass capillaries. Samples for collection at high temperature were packed into 0.3 mm quartz capillaries. Data were collected in the 2θ range 3–83 ° in two frames shifted by 0.5 ° in order to cover the 0.2 ° gaps between the modular detectors every 5 °. High temperature data were collected using the hot air blower attachment (300 K – 1248 K) and low temperature data were collected using the cyrostream attachment (90 K – 300 K).

3. Results

3.1 Composition range of the $\text{Sr}_{1-x}\text{Ti}_{1-2x}\text{Nb}_{2x}\text{O}_3$ series

The composition range of the $\text{Sr}_{1-x}\text{Ti}_{1-2x}\text{Nb}_{2x}\text{O}_3$ series has been carefully re-investigated. Previous results were somewhat contradictory and interpretations were based on laboratory X-ray diffraction rather than high resolution synchrotron X-ray or neutron powder diffraction [4–7]. The composition range can be divided into roughly three portions (see Figure 1).

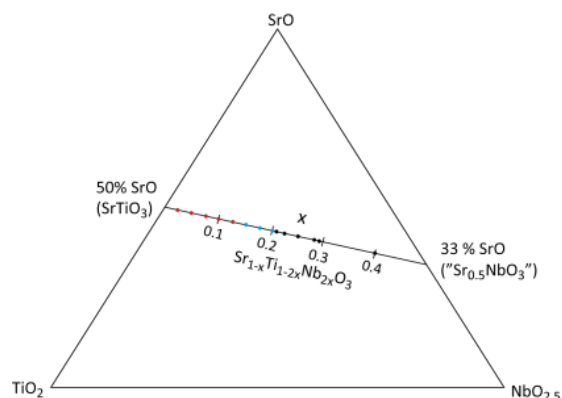


Fig. 1. Partial SrO-TiO₂-NbO_{2.5} phase diagram highlighting the existence of the $\text{Sr}_{1-x}\text{Ti}_{1-2x}\text{Nb}_{2x}\text{O}_3$ series.

In the region $0 \leq x \leq 0.125$ (red dots) we find the cubic $Pm\bar{3}m$ $\text{Sr}_{1-x}\text{Ti}_{1-2x}\text{Nb}_{2x}\text{O}_3$ solid solution with minor intergrowth of SrTiO_3 . Between $0.125 < x \leq 0.2$ (blue dots) we can always get the pure solid solution phase, while at higher vacancy concentrations (black dots) the $x = 0.2$ end member and the $\text{Sr}_3\text{TiNb}_4\text{O}_{15}$ tungsten bronze are formed. This is in contrast to the related $\text{Sr}_{1-x}\text{Zr}_{1-2x}\text{Nb}_{2x}\text{O}_3$ phases, where x can be as high as ~ 0.28 , but the symmetry changes from $Pnma$, to $Imma$ and $I4/mcm$ with increasing vacancy concentration.

3.2. Synchrotron X-ray Powder Diffraction of $\text{Sr}_{1-x}\text{Ti}_{1-2x}\text{Nb}_{2x}\text{O}_3$ ($0 \leq x \leq 0.2$)

Synchrotron X-ray powder diffraction patterns were collected for all compositions synthesised in the region $0 \leq x \leq 0.2$. In the samples from region 1 reflections attributed to SrTiO_3 persisted, but no additional superlattice reflections were observed in any of the patterns. This lack of additional superlattice reflections suggests that the structure of the $\text{Sr}_{1-x}\text{Ti}_{1-2x}\text{Nb}_{2x}\text{O}_3$ series is identical to that of the end member SrTiO_3 , that is, an ideal cubic

perovskite. Thus, the best fit and most stable refinement obtained for all of the structures in the $\text{Sr}_{1-x}\text{Ti}_{1-2x}\text{Nb}_{2x}\text{O}_3$ ($0 \leq x \leq 0.2$) series applied the space group symmetry $Pm\bar{3}m$ (see Figure 2). All Rietveld refinements were carried out using the Jana2006 package [8].

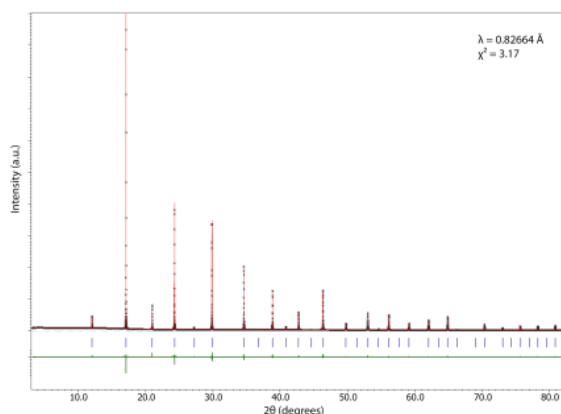


Fig. 2. X-ray powder diffraction pattern for the $\text{Sr}_{0.8}\text{Ti}_{0.6}\text{Nb}_{0.4}\text{O}_3$ sample collected at the Australian Synchrotron ($\lambda = 0.82664 \text{ \AA}$; space group $Pm\bar{3}m$).

The ideal bond lengths of Nb^{5+} (1.965 \AA) and Ti^{4+} (1.978 \AA) to oxygen in octahedral coordination, as determined via bond valence sums [9], are roughly equivalent so substitution of one for the other should cause little disruption to the structure. This however, does not consider the effects of the vacancies produced in substituting Nb^{5+} for Ti^{4+} . The generation of a vacancy leads to the surrounding oxygen anions becoming partially under-bonded. In this circumstance, the oxygen anions shift slightly closer to adjacent strontium cations to maintain their bonding requirements. Thus, it was expected that, with the combination of *B* cations and vacancies on the A-site, distortions may be occurring locally without periodically translating to long range order. Such short range order would result in diffuse scattering, which should be observable in electron diffraction patterns. These octahedral rotations, even if only on a local scale, would still lead to lower than expected thermal expansion.

3.3 Thermal expansion of $\text{Sr}_{1-x}\text{Ti}_{1-2x}\text{Nb}_{2x}\text{O}_3$ ($x = 0.2$)

Variable temperature synchrotron X-ray powder diffraction data have been collected for $\text{Sr}_{1-x}\text{Ti}_{1-2x}\text{Nb}_{2x}\text{O}_3$ ($x = 0.2$) from 90 K – 1248 K. Figure 3 shows the evolution of the cubic cell dimension over this temperature range.

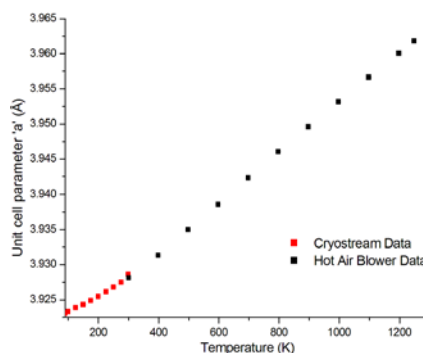


Fig 3. Cell parameters for $\text{Sr}_{0.8}\text{Ti}_{0.6}\text{Nb}_{0.4}\text{O}_3$ from 90 K – 1298 K.

The thermal expansion coefficient calculated from these data is $\alpha = 8.72(9) \times 10^{-6} \text{ K}^{-1}$, which is significantly smaller than the value of $\alpha = 3.23(2) \times 10^{-5} \text{ K}^{-1}$ for the $x = 0$ end

member, *i.e.* SrTiO₃. This result suggests that the octahedral rotations are more prominent in Sr_{0.8}Ti_{0.6}Nb_{0.4}O₃ than in the parent compound SrTiO₃. This can be explained by considering what occurs to the size of the unit cell when octahedral tilting occurs. For an ideal cubic perovskite the Ti/Nb-O-Ti/Nb bond angle is 180°. If the structure is slightly distorted, however, this angle begins to deviate away from 180°. As the structure is heated then an increase in the lattice vibrations will lead to a greater deviation from 180° on average. As the angle deviates further from 180°, the distance between adjacent B-site cations will decrease, reducing the expansion of the unit cell. It would thus appear that the A-site vacancies allow stronger octahedral rotation, without locking into a lower symmetry phase.

3.4 Lithium intercalation investigations

Lithium intercalation into the Sr_{0.8}Ti_{0.6}Nb_{0.4}O₃ phase was performed using n-butyllithium in boiling hexane for up to 7 days. The resulting phase changed colour from white to blue-grey and was analysed using synchrotron powder X-ray diffraction and inductively coupled plasma atomic emission spectroscopy (ICP-AES). Both techniques indicate that a small amount of lithium was incorporated. The cell dimension changes from 3.928021(1) to 3.928831(1) Å and the molar mass increases from 183.98 for Sr_{0.8}Ti_{0.6}Nb_{0.4}O₃ (calculated) to 184.5 for Li_ySr_{0.8}Ti_{0.6}Nb_{0.4}O₃ as determined from ICP-AES ($y = 0.075(1)$). In contrast Sr_{0.75}Zr_{0.5}Nb_{0.5}O₃ has been shown to intercalate up to $y = 0.5$ Li per formula unit on electrochemical intercalation in a swagelock cell [10].

Conclusions

The series of defect perovskites show differences in both structure and lithium intercalation properties. The Sr_{1-x}Zr_{1-2x}Nb_{2x}O₃ ($0 \leq x \leq 0.28$) system has a wider composition range, but shows a series of phase transitions, while the Sr_{1-x}Ti_{1-2x}Nb_{2x}O₃ ($0 \leq x \leq 0.2$) analogue has a somewhat narrower composition range, but does form a cubic solid solution. The highest concentration of vacancies, however, in the titanium phase seems to be too low to allow effective lithium intercalation, while the zirconium compound with the highest vacancy concentration intercalates lithium quite readily. Further investigations will aim to improve the properties of the titanium system by stabilising a phase with nominally higher numbers of vacancies on the A-site.

Acknowledgments

The authors thank Dr Qinfen Gu for assistance collecting powder diffraction data at the Australian Synchrotron and the Australian Synchrotron for financial assistance.

References

- [1] Hessen B, Sunshine S A, Siegrist T, Jimenez R 1991 *Mat. Res. Bull.* **26** 85
- [2] Schmid S, Elcombe M, Rhode M 2006 *Australian Institute of Physics, Conference Proceedings 'Wagga 2006'* ISBN 1-920791-09-4, TP15
- [3] Schmitt B, Brönnimann C, Eikenberry E F, Gozzo F, Hörmann C; Horisberger R, Patterson B 2003 *Nucl. Instrum. Methods A* **501** 267
- [4] Thangadurai V, Shukla A K, Gopalakrishnan J 1999 *Chem. Mater.* **11** 835
- [5] Irvine J T S, Slater P R, Wright P A 1996 *Ionics* **2** 213
- [6] Kolodiaznyi T, Petric A 2005 *J. Electroceram.* **15** 5
- [7] Tien T-Y, Moratis C J 1967 *J. Am. Ceram. Soc.* **50** 392
- [8] Petříček V, Dušek M, Palatinus L 2006 *Jana2006*, The crystallographic computing system, Institute of Physics, Praha, Czech Republic
- [9] Brown I D, Altermatt D 1985 *Acta Crystallogr.* **B41** 244
- [10] Schmid S and Kuhn A, Manuscript in preparation